



# Experimental Observations on a Suction Bucket Foundation Under Vertical Pullout Loading

Sung-Ryul Kim<sup>(✉)</sup>, Seongho Hong, and Ssenyondo Vicent

Department of Civil and Environmental Engineering,  
Seoul National University, Seoul, South Korea  
sungryul@snu.ac.kr

**Abstract.** The government of South Korea is currently implementing the national plan of developing offshore wind energy in the southwestern sea of the Korean peninsula. The aim is to decrease the nation's consumption of carbon emission technologies and increase renewable energy consumption. A tripod bucket foundation has been identified as a feasible foundation to support offshore wind turbine structures. This type of foundation is subject to failure by moment, horizontal, and pullout loadings due to the impact of wind and wave loads. The pullout of one bucket determines the stability of the entire tripod system, and should be investigated to fully satisfy the applicability of the tripod bucket foundation in the ongoing campaign. Therefore, a series of 1-g experimental tests were conducted on the model suction bucket to evaluate the pullout capacity under drained and undrained conditions. Soil deformations outside the bucket, soil heave, and suction force inside the bucket are discussed. A simple approach is proposed to guide the pullout capacity evaluation under drained and undrained conditions.

**Keywords:** Suction bucket · 1-g experimental test · Drainage condition · Pullout capacity · Sand

## 1 Introduction

In response to the United Nation's requirement for countries to mitigate greenhouse gas emissions, the South Korean government plans to increase renewable energy production from 4.8% to 20% by 2030 [1]. The latest 8th basic plan of South Korea for power supply and demand shows that offshore wind power is expected to contribute 23% of the total renewable energy production by 2030 [2]. The South Korean government, through the Ministry of Trade, Industry, and Energy, is currently progressively promoting the construction of offshore wind farms in the southwestern sea of the Korean peninsula. The development plan (Fig. 1) comprises the following three phases: phase 1-verification (2011–2018), phase 2-demonstration (2018–2020), and phase 3-expansion (2020–). This plan will increase the offshore wind capacity of the nation from the current 124 MW to 12 GW by 2030 [3]. The construction of 400 MW and 2 GW plants is scheduled to commence in 2022 and 2023, respectively. Nearly 2.46 GW will be generated by 2028, which is sufficient to supply electricity to 2.24 million households. Site investigations

revealed that the southwestern sea is an ideal site for wind power generation due to favorable wind speeds ( $>6.9$  mm/s), shallow to deep waters (10–60 m), and short distances from the on-land sub stations [4].



**Fig. 1.** Development plan for offshore wind power projects in Korea [5].

A tripod bucket foundation has been identified as a feasible foundation to support offshore wind turbine structures [5]. The tripod bucket foundation is subject to failure by moment, horizontal, and pullout loadings due to the impact of wind and wave loads. The moment and horizontal capacities of the tripod bucket in this offshore environment have been addressed by previous studies. The pullout of a bucket in the tripod bucket foundation governs the stability of the entire tripod bucket system [6]. The pullout of one bucket can destabilize the entire tripod group, ultimately causing the breakdown of the entire foundation system. Figure 2 shows an illustration of the tripod bucket failure. The uplifting bucket is subjected to tension, while the downward buckets are subjected to compression. Therefore, evaluating the pullout capacity of the suction bucket is necessary. Moreover, the bucket has the least resistance to pullout when the pullout load acts in the vertical direction [7]. Tran et al. [8] discussed the relationship between the pullout and moment capacities of the bucket. The moment capacity can be calculated by considering the spacing of buckets, the pullout capacity of the upward bucket, and the vertical weight of the wind turbine structure.

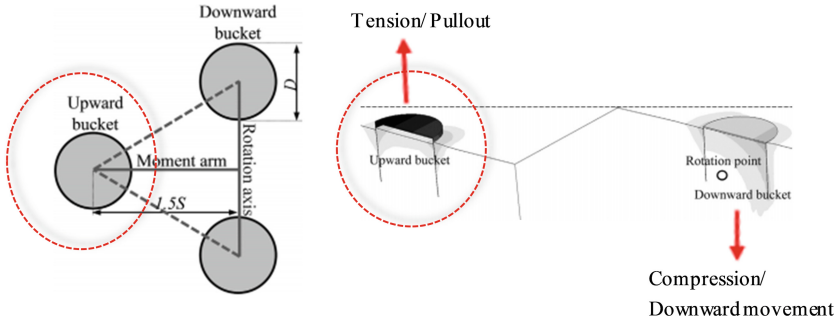


Fig. 2. Failure mechanism of a tripod bucket system [8].

## 2 Previous Studies on Pullout Capacity

The pullout capacity is considerably affected by the drainage condition of soils surrounding the bucket. Drainage conditions include drained, partially drained, and undrained conditions. Figure 3 shows failure modes of the bucket under the aforementioned drainage conditions. The drainage condition is influenced by suction developed inside the bucket during bucket pullout. This suction depends on factors, such as loading rate, drainage length, hydraulic conductivity, and shear strength properties of the soil [9].

A drained condition is induced by slow loading rates [10]. The suction pressure generated inside the bucket is substantially small under this drainage condition such that no soil is uplifted inside the bucket. The bucket resists uplift by friction resistance of the inner and outer faces of the bucket skirt. The skin resistance increases with the increase in friction angle of soil. Analysis of data from a centrifuge test study on model suction bucket foundations revealed that drained pullout capacity increases as a power function of bucket embedment depth at constant diameter [11]. The drained pullout capacity equals to the summation of the total skin resistance and the submerged weight of the bucket and its components because the bucket is pulled out by the sliding of the inner and outer faces of the bucket skirt [9, 12]. An accurate prediction of drained pullout capacity can be obtained by applying the equations proposed by Houlsby et al. [13], which account for the reduction of the vertical effective stress close to the bucket. The reduction of effective stress is due to friction forces along the bucket.

A partially drained condition, which exists between drained and undrained conditions, is characterized by partial uplift of the soil plug. A gap may form under the lid during the uplift of the bucket. Seepage into this gap leads to loss of suction. The generated suction increases with the loading rate, thus raising the volume of entrapped soil [14]. The pullout capacity under partially drained conditions can be predicted by summing up the submerged weight of the bucket, bottom resistance, and the outer skirt resistance [12]. Previous studies proposed that the pullout capacity in sandy ground can be predicted by equations suggested by Houlsby et al. [13]. The equations apply a factor to suction measured below the lid of the bucket. The factor accounts for the skin friction coefficient ( $K_{tan}\delta$ ) and the change in embedment depth.

The undrained condition occurs at rapidly fast loading rates, which hinder the dissipation of suction. Gap formation under the lid is absent under undrained condition, and

all soil trapped inside the bucket uplifts with the bucket. The pullout capacity increases as the uplifted soil plug volume increases. The generated suction force also increases and may contribute over 60% of the pullout capacity [15]. Previous studies suggested several models to evaluate the undrained pullout capacity. These models are summarised by the studies of Thorel et al. [16] and Patel and Singh [17]. The majority of these models were developed from studies on clay grounds (e.g., [18, 19]); therefore, their application to buckets in sandy ground might be limited. The general expression for undrained pullout capacity of a cylindrical caisson can guide the prediction of undrained bearing capacity in sandy ground [9]. The undrained pullout capacity is equal to the sum of submerged weights for the bucket and soil plug, the bottom resistance, and the outer skin resistance of the bucket. The outer skin resistance is calculated using the effective stress approach considering the increase in effective stress due to seepage along the outer skirt. The undrained pullout, which is a reversed end-bearing failure, and can be theoretically evaluated by applying the reversed bearing capacity theory [12]. Previous studies predicted that the undrained pullout capacity is approximately three times larger than the drained pullout capacity [9, 17]. Sandy ground occupies a considerable portion of the current project site. Until now, information to support the evaluation of pullout capacities in sandy ground is limited. [9, 20, 21]. Further studies are necessary to develop simplified solutions that can guide the prediction of the pullout capacity.

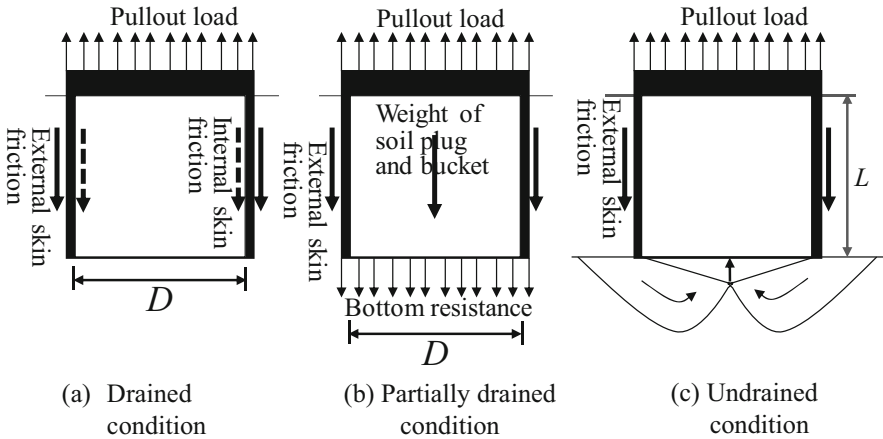


Fig. 3. Failure modes of the bucket during pullout loading (Modified after [12]).

### 3 Pullout Capacity According to Drainage Condition

A series of 1-g experimental tests were conducted on a single model bucket to evaluate the pullout capacity. The pullout load of the bucket was varied by applying different loading rates to induce bucket pullout under drained partially drained and undrained conditions. Soil heave and suction force inside the bucket are comprehensively discussed, and a simple approach is proposed to guide the pullout capacity evaluation under drained and undrained conditions.

### 3.1 Model Preparation and Testing

Figure 4 shows bucket models applied in the current study. Experimental data were obtained by applying the aluminum bucket. The polycarbonate bucket was purposely applied to enable visualization and monitoring of soil heave phenomena inside the bucket during the pullout process.

The aluminum model bucket had a Young's modulus ( $E = 70$  Gpa), lid and skirt thicknesses of 5 and 1 mm, respectively. The model dimensions were obtained by scaling down geometric parameters of a commonly used steel prototype bucket ( $E = 210$  Gpa) with  $L/D = 1.0$  ( $L = 15$  m). The scaling laws proposed by Wood [22] were adopted by applying the geometric scale ratio of 1:100 for length. The soil box had a diameter of 600 mm and height of 450 mm. Preliminary finite element analyses proved that, the boundary extents of the soil box had no effect on the pullout capacity. The model ground was saturated loose silica sand with the following properties: mean grain size ( $D_{\text{mean}} = 0.11$  mm), permeability ( $k = 2.51 \times 10^{-4}$  m/s), relative density ( $D_r = 28\%$ ) and specific gravity ( $G_s = 2.65$ ).

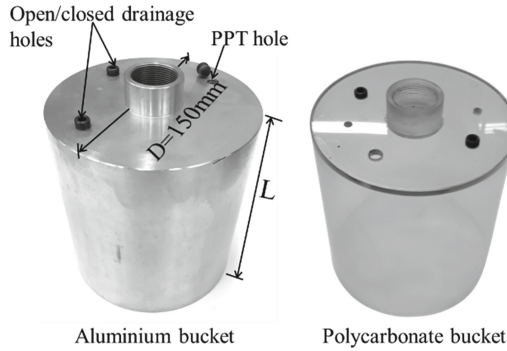


**Fig. 4.** Model suction bucket ( $L/D = 1.0$ ).

Dry sand was initially submerged in water and allowed to saturate completely for a period of at least 48 h [23]. The model ground was prepared by pluviating saturated sand particles in water [24, 25] using the following procedure. A sieve (ASTM No. 40) was stacked on top of the soil box shown in Fig. 5. The soil box was filled with water, ensuring that the mesh is fully submerged. Saturated sand was dispersed over the submerged mesh. The sand particles dropped in water and settled with a uniform velocity inside the soil box. The model ground was loose with an average relative density ( $D_r$ ) and saturated unit weight ( $\gamma_{\text{sat}}$ ) equal to 28% and 17.3 kN/m<sup>3</sup>, respectively). The same procedures were adopted to make the model ground for each experimental test. Drainage holes on the lid of the bucket were opened, and the bucket was slowly pushed into the ground at an average velocity of 0.0625 mm/s, which was sufficiently slow to limit excess pore water pressure generation in the soil. Bucket penetration was stopped when the lid touched the ground surface.

Figure 5 shows the test set-up used to conduct the experimental tests. The test equipment applied the load-controlled method. This test set-up was adopted because it allows

the implementation of extremely slow loading rates e.g. 0.004 N/s. Extremely slow loading rates are difficult to implement using the existing test methods. The instrumentation included two linear variable differential transformers to measure bucket displacement, a load cell to measure the pullout load, and pore pressure transducers to measure suction pressure developed inside and below the bucket during uplift. A loading wire was set to pass over the pulley system connecting the bucket on one end while suspending the loading container on the other end. The control valve was opened to induce bucket pullout load and regulate a uniform flow of water into the loading container. As water accumulated in the loading container, the tension in the loading wire increased, thus applying a pullout force on the bucket. The above procedure was repeated for all loading rates in the test program. The test program was designed to apply loading rates of 0.004, 0.008, 0.08, 0.66, and 2.05 N/s.

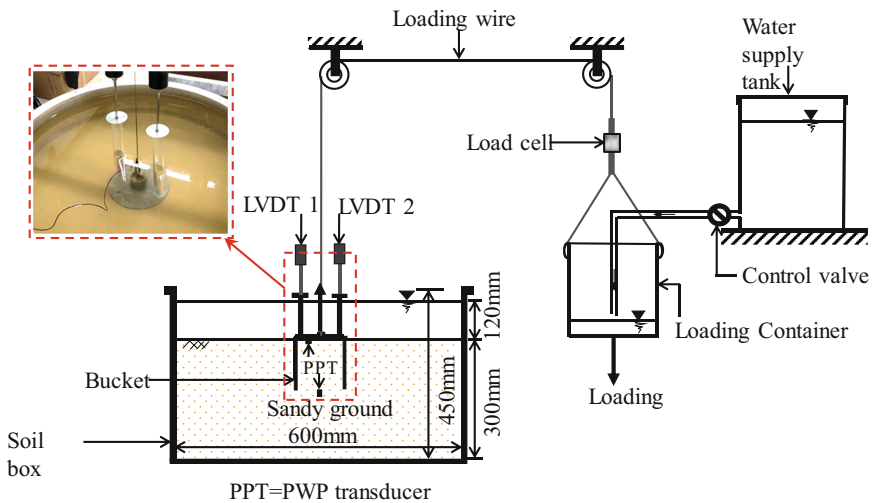


Fig. 5. Set-up of the test equipment for bucket pullout loading.

### 3.2 Results and Discussions

**Pullout Capacity Considering Drainage Condition.** Figure 6 shows the pullout load versus pullout displacement ( $w/D$ ), where  $w$  is the upward displacement and  $D$  is the bucket diameter. The skin resistance is considerably mobilized at the onset of load application. When the pullout load exceeds some critical value, large displacements occur at small increments in pullout load. Figure 7 shows the suction pressure generated below the lid and tip of the bucket. The generated suction depends on the magnitude of applied loading rate. The larger the loading rate, the larger the generated suction force. The trend for the increase of suction force below the lid was similar to that of the load–displacement curve, indicating that the generated suction force governs the pullout resistance. The bottom suction resistance increased with the suction inside the bucket.

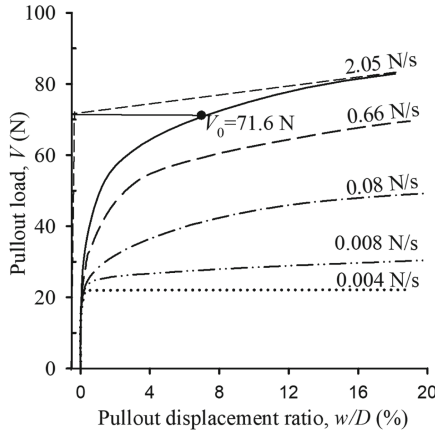


Fig. 6. Pullout load-displacement curves of the bucket.

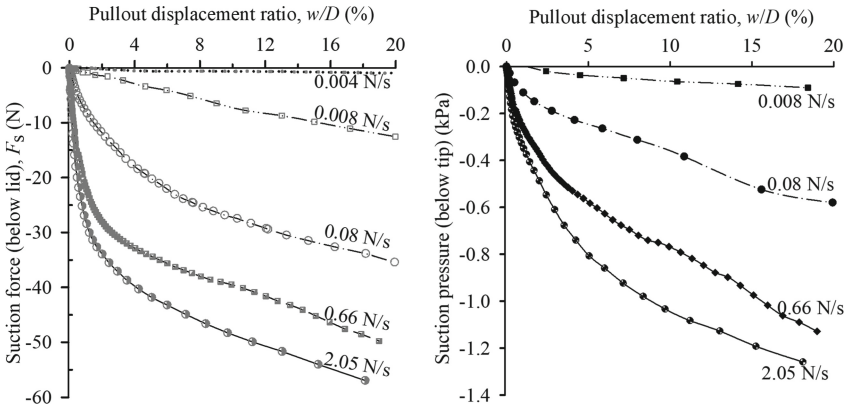


Fig. 7. Suction force below the lid and tip of the bucket.

The tangent intersection method was applied to estimate the pullout capacity ( $V_0$ ) as illustrated in Fig. 6 [26, 27]. The displacement at  $V_0$  was recorded and applied to estimate the suction force ( $F_{s0}$ ) mobilized at pullout capacity. Figure 8 shows the increase of suction force during uplift. The suction force inside the bucket was not constant during bucket pullout for each loading rate, but increased with bucket uplift as shown at displacement ratios ( $w/D$ ) of 3.3%, 10%, and 16%.

Figure 9 shows the variation of pullout capacities ( $V_0$ ) and suction force ( $F_{s0}$ ) with loading rate. The pullout capacity rapidly increased with loading rate from 0.004 N/s to 0.66 N/s. However, over 2.05 N/s indicates the absence of significant changes in the pullout capacity. The rapid increase in pullout capacity was due to the increase in suction force generated inside the bucket. The experimental data are plotted as shown in Fig. 9. A curve defined by a hyperbolic function was found to best fit experimental data. The drained pullout capacity ( $V_d$ ) was 22.1 N and occurred at a loading rate of 0.004 N/s with negligible suction force. The undrained pullout capacity ( $V_u$ ), the lid suction ( $F_{su(lid)}$ ),

and the tip suction ( $F_{su(\text{bottom})}$ ) were estimated to be 75, 48.3, and 18.1 N, respectively. The undrained pullout capacity occurred at loading rates larger than 2.05 N/s.

Table 1 summarizes the pullout capacities, top and bottom suction forces, and the percentage contribution of suction on pullout capacity. The suction force inside the bucket mainly contributed to the increase in pullout capacity at loading rates larger than 0.66 N/s.

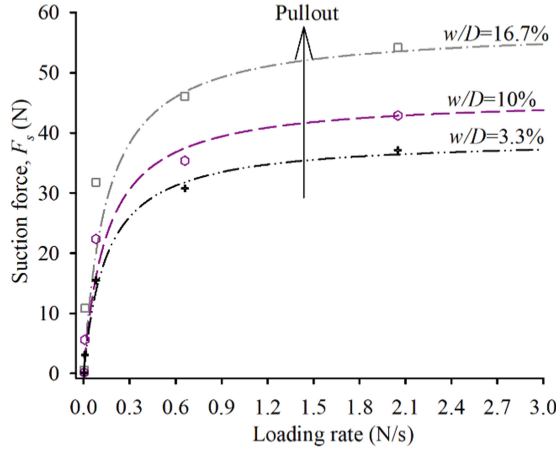


Fig. 8. Example of the increase in suction force (under lid) during bucket uplift.

Table 1. Pullout capacity and suction force inside the buckets.

Loading rate (N/s)	$V_0$ (N)	$F_{s(\text{lid})}$ (N)	$F_{s(\text{tip})}$ (N)	$F_{s(\text{lid})}/V_0$	$F_{s(\text{tip})}/V_0$ (%)
0.004	22.1	$\approx 0$	$\approx 0$	$\approx 0$	$\approx 0$
0.008	26.66	3.34	1.32	12.53	10.54
0.08	41.97	18.51	5.11	44.10	11.59
0.66	57.07	32.53	10.06	57	17.65
2.05	71.6	44.48	15.92	62.12	25.63

As previously discussed, the suction pressure increased with the loading rate. The suction pressure below the bucket tends to resist uplift, but its percentage contribution to pullout capacity is small compared with the suction effects under the lid. Figure 9 shows a simple evaluation in which the sum of  $F_{su(\text{lid})}$ ,  $F_{su(\text{tip})}$ , and  $R_{s(\text{outer skirt})}$  is approximately equal to  $V_u$ .  $R_{s(\text{outer skirt})}$  is estimated to be half of the difference between  $V_d$  and submerged bucket weight ( $W_b' = 7.61$  N).

**Drained ( $V_d$ ) and Undrained ( $V_u$ ) Pullout Capacities.** Figure 10 shows the heaving of soil inside the bucket during pullout. The drained condition is observed in Fig. 10a,

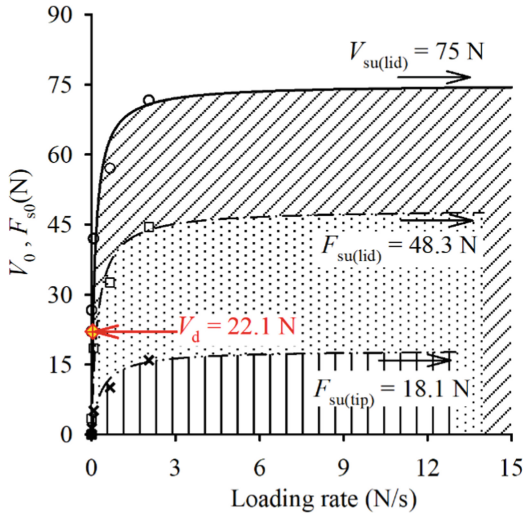


Fig. 9. Drained and undrained pullout capacities from the experimental test data.

which shows an empty bucket pullout. When the skin friction is exceeded, the bucket rapidly uplifts without the soil plug, and no settlement takes place in the soil surrounding the bucket. The drained pullout capacity can be evaluated by applying Eq. (1). The undrained condition is demonstrated in Fig. 10b, which shows that all the entrapped soil uplifts with the bucket. The mobilized suction force is larger than the weight of the soil plug. When a full soil plug was uplifted, the measured tip suction was approximately 50% of lid suction.

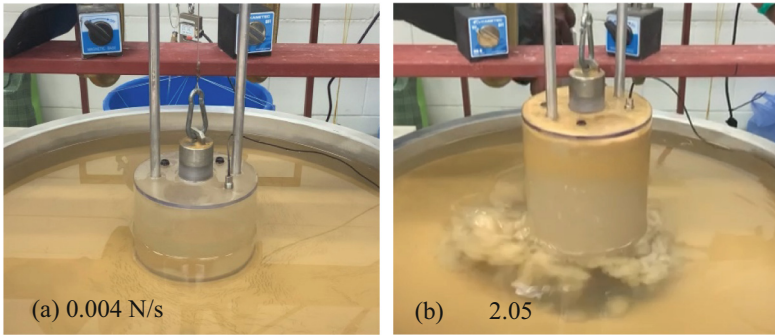


Fig. 10. Bucket pullout at slow and fast loading rates.

$$V_0 = R_{s(\text{outer skirt})} + R_{s(\text{inner skirt})} + W_b' \tag{1}$$

where  $R_{s(\text{outer skirt})} = R_{s(\text{inner skirt})} = \frac{\gamma' L}{2} \times K \tan \delta \times \pi \times D \times L$ ,  $\gamma'$  is the effective unit weight of soil,  $K$  = lateral earth pressure coefficient, and  $\delta$  is the soil–bucket skirt

interface angle of friction. The submerged weight of the bucket ( $W_b'$ ) is 7.61 N, and  $K \tan \delta$  is estimated as 0.182.

Figure 11 shows the balance of forces acting on the bucket during undrained pullout loading. The bucket with soil act as one body during the undrained pullout. The undrained pullout capacity can be estimated by applying Eq. (2). The maximum tensile force ( $F_{s(\text{bottom})}$ ) is assumed to be limited to the buoyancy at the bottom of the bucket ( $\gamma_w LA$ ). It is also assumed that the increase in  $R_{s(\text{outer skirt})}$  due to downward seepage force equals to the decrease in  $R_{s(\text{inner skirt})}$ .

$$V_u = W_b + W_{\text{soil}} + R_s + (\gamma_w \times H \times A) - (\gamma_w \times H \times A + \gamma_w \times L \times A) + F_{s(\text{bottom})}$$

$$V_u = W_b + W_{\text{soil}} + R_s - (\gamma_w \times L \times A) + F_{s(\text{bottom})} \quad (2)$$

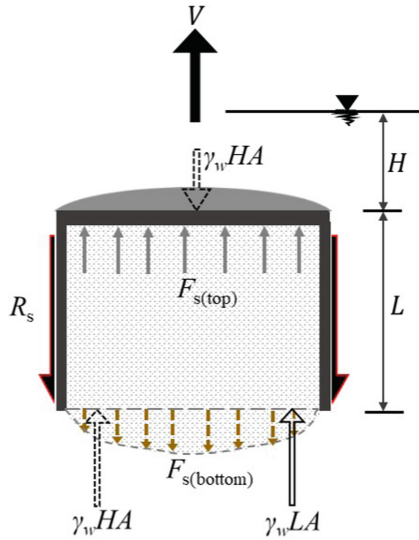


**Fig. 11.** Forces acting on the bucket during undrained pullout loading.

where  $W_b$  and  $W_s$  are the respective weights for the bucket and soil,  $F_{s(\text{bottom})}$  is the suction force at the bottom of the bucket,  $H$  is the water level from the top of the bucket, and  $L$  is the height of the bucket. The water pressure at the bottom of the bucket is equal to  $\gamma_w \times (H + L) \times A$ . At the ultimate pullout limit state,  $F_{s(\text{bottom})}$  is equal to  $\gamma_w \times L \times A$ , and the ultimate pullout capacity can be estimated by applying Eq. (3).

$$V_u = W_b + W_{\text{soil}} + R_s \quad (3)$$

$R_s$  considers the  $R_{s(\text{outer skirt})}$  and  $F_{\text{seepage}}$ .  $F_{\text{seepage}}$  is assumed equal to  $R_{s(\text{inner skirt})}$ , and  $V_u$  can be predicted by applying Eq. (4).

$$V_u = W_b + W_{\text{soil}} + R_{s(\text{inner skirt})} + R_{s(\text{outer skirt})} \quad (4)$$

where  $W_b$  and  $W_{\text{soil}}$  are the respective weights for the bucket and trapped soil, and  $R_S$  can be evaluated by applying  $K \tan \delta = 0.182$ .

Equation 4 predicted  $V_u = 68.9$  N, while Fig. 11 (Hyperbolic fit) predicted  $V_u = 75$  N. The percentage difference between the two values is 8.5%, which is less than 10%. Therefore, Eq. (4) can be used to obtain a reasonable estimate for  $V_u$ .

The current study has a number of limitations. The bucket models of the current study are small and besides, experimental tests were conducted under 1-g conditions. As expected, the pullout loads are smaller compared to those usually encountered in field practice. Therefore, the effects of cavitation on the pullout capacity of model buckets are insignificant. In typical offshore bucket foundations, large pullout loads impact the suction bucket. The cavitation of the pore fluid beneath the bucket significantly limits the increase of pullout capacities at larger loading rates. Cavitation of the pore fluid is estimated to occur at a pressure of  $-100$  kPa. Furthermore, bucket foundations are subjected to cyclic loads of wind and waves of various magnitudes. Factors that affect the cyclic response e.g. load inclination and number of cycles are not addressed by the current study.

## 4 Conclusion

This study discussed experimental observations and findings on the pullout capacity of a single bucket by conducting a series of 1-g experimental tests. The pullout load of the bucket was varied by applying different loading rates to induce bucket pullout under drained to undrained conditions. The following conclusions are drawn.

The tripod bucket foundation is a feasible foundation for offshore wind turbines in the southwestern sea of the Korean Peninsula. The tripod bucket foundation is subject to failure by moment, horizontal, and pullout loadings. The pullout capacity of a single bucket governs the design of a stable tripod bucket system.

The pullout capacity is significantly affected by the drainage condition of the soil surrounding the bucket. A drained condition is induced by a slow loading rate, and the suction force generated in the soil is substantially small and negligible. The undrained condition is induced by a fast loading rate. The suction force generated is large, which provides remarkable contributions to the pullout capacity. The partially drained condition, which exists between the drained and undrained conditions, is induced by intermediate loading rates. As the loading rate increases, the pullout capacity increases proportionally to the induced suction force.

The drained pullout capacity can be predicted by combining skin resistances along the inner and outer bucket skirts and the submerged weight of the bucket. Meanwhile, the undrained pullout capacity can be estimated by combining the soil plug weight, bucket weight, and the inner and outer skirt resistances of the bucket.

**Acknowledgement.** This work was supported by Research Resettlement Fund for the new faculty of Seoul National University and the Development of Life-cycle Engineering Technique and Construction method for Global competitiveness upgrade of Cable bridges (16SCIP-B119960) from the Smart Civil Infrastructure Research Program funded by the Ministry of Land, Infrastructure and Transport (MOLIT) of the Korean Government and the Korea Agency for Infrastructure Technology Advancement (KAIA).

## References

1. Park, J., Kim, B.: An analysis of South Korea's energy transition policy with regards to offshore wind power development. *Renew. Sustain. Energy Rev.* **109**, 71–84 (2019)
2. Park, J., Kim, B.: A comparative study on government's policy for offshore wind power development between major European country and Korea. *New Renew. Energy* **15**(3), 11–26 (2019)
3. MOTIE Homepage. [http://www.motie.go.kr/motie/ne/presse/press2/bbs/bbsView.do?bbs\\_cd\\_n=81&bbs\\_seq\\_n=160584](http://www.motie.go.kr/motie/ne/presse/press2/bbs/bbsView.do?bbs_cd_n=81&bbs_seq_n=160584). Accessed 27 Nov 2020
4. Kim, J.Y., Kang, K.S., Oh, K.Y., Lee, J.S., Ryu, M.S.: A study on the site selection of offshore wind farm around Korean Peninsula. In: *Proceedings of the 3rd International Conference on Ocean Energy, ICOE 2010, Bilbao, Spain* (6), pp. 1–4 (2010)
5. Ryu, M.S., Lee, J.S., Kwag, D.J., Bang, S.: Comparison of two meteorological tower foundations for off-shore wind turbines. In: *Proceedings of the 26th International Ocean and Polar Engineering Conference*, pp. 723–730. International Society of Offshore and Polar Engineers, Rhodes (2016)
6. Kim, S.R., Oh, M.: Group effect on bearing capacities of tripod bucket foundations in undrained clay. *Ocean Eng.* **79**, 1–9 (2014)
7. Rao, S.N., Latha, K.H., Pallavi, B., Surendran, S.: Studies on pullout capacity of anchors in marine clays for mooring systems. *Appl. Ocean Res.* **28**(2), 103–111 (2006)
8. Tran, N.X., Hung, L.C., Kim, S.R.: Evaluation of horizontal and moment bearing capacities of tripod bucket foundations in sand. *Ocean Eng.* **140**, 209–221 (2017)
9. Iskander, M., El-Gharbawy, S., Olson, R.: Performance of suction caissons in sand and clay. *Can. Geotech. J.* **39**(3), 576–584 (2002)
10. Vicent, S., Kim, S.R., Tung, D.V., Bong, T.: Effect of loading rate on the pullout capacity of offshore bucket foundations in sand. *Ocean Eng.* **210**, 107427 (2020)
11. Wang, X., Zeng, X., Li, J.: Vertical performance of suction bucket foundation for offshore wind turbines in sand. *Ocean Eng.* **180**, 40–48 (2019)
12. Deng, W., Carter, J.P.: A theoretical study of the vertical uplift capacity of suction caissons. *Int. J. Offshore Polar Eng.* **12**(02), 89–97 (2002)
13. Houlsby, G.T., Kelly, R.B., Byrne, B.W.: The tensile capacity of suction caissons in sand under rapid loading. In: *Proceedings of the International Symposium on Frontiers in Offshore Geomechanics*, pp. 405–410. Taylor & Francis Group, Perth (2005)
14. Thieken, K., Achmus, M., Schröder, C.: On the behavior of suction buckets in sand under tensile loads. *Comput. Geotech.* **60**, 88–100 (2014)
15. Clukey, E.C., Morrison, M.J.: A centrifuge and analytical study to evaluate suction caissons for TLP applications in the Gulf of Mexico. In: *Design and Performance of Deep Foundations: Piles and Piers in Soil and Soft rock*, ASCE, pp. 141–156 (1993)
16. Thorel, L., Garnier, J., Rault, G., Bisson, A.: Vertical uplift capacity of suction caisson in clay. In: *Proceedings of the International Symposium on Frontiers in Offshore Geotechnics (IS-FOG 2005)*, pp. 273–279 (2005)
17. Patel, S.K., Singh, B.: A parametric study on the vertical pullout capacity of suction caisson foundation in cohesive soil. *Innov. Infrastruct. Solut.* **4**(1), 1–11 (2018). <https://doi.org/10.1007/s41062-018-0188-6>
18. Rahman, M.S., Wang, J., Deng, W., Carter, J.P.: A neural network model for the uplift capacity of suction caissons. *Comput. Geotech.* **28**(4), 269–287 (2001)
19. Sgardeli, C.G.: A finite element analysis of the pullout capacity of suction caissons in clay (Doctoral dissertation, Massachusetts Institute of Technology) (2009)
20. Sawicki, A., Wachowski, Ł., Kulczykowski, M.: The pull-out capacity of suction caissons in model investigations. *Arch. Hydro-Eng. Environ. Mech.* **63**(2–3), 157–171 (2016)

21. Hung, L.C., Lee, S., Tran, N.X., Kim, S.R.: Experimental investigation of the vertical pullout cyclic response of bucket foundations in sand. *Appl. Ocean Res.* **68**, 325–335 (2017)
22. Wood, D.M.: *Geotechnical Modelling*, pp. 246–268. CRC Press, Boca Raton (2004). Reference to (Chapter 5)
23. Vicent, S., Hung, L.C., Kim, S.R.: Effects of long-term cyclic horizontal loading on bucket foundations in saturated loose sand. *Appl. Ocean Res.* **91**, 101910 (2019)
24. Kim, S.R., Jang, I.S., Chung, C.K., Kim, M.M.: Evaluation of seismic displacements of quay walls. *Soil Dyn. Earthq. Eng.* **25**(6), 451–459 (2005)
25. Vaid, Y.P., Negussey, D.: Preparation of reconstituted sand specimens. In: *Advanced Triaxial Testing of Soil and Rock*. ASTM International, pp. 405–417 (1988)
26. Vicent, S., Hung, L.C., Kim, S.R.: Evaluation of horizontal and vertical bearing capacities of offshore bucket work platforms in sand. *Appl. Ocean Res.* **101**, 102198 (2020)
27. Graham, J., Pinkney, R.B., Lew, K.V., Trainor, P.G.S.: Curve-fitting and laboratory data. *Can. Geotech. J.* **19**, 201–205 (1982)